Chapter 8
Conclusion

We conclude with a presentation of confidence intervals bounding the relative importance of weak annihilation and a discussion of where we might go from here.

8.1 Limits on Significance of Weak Annihilation

We have studied inclusive charmless semileptonic B decays with the purpose of constraining the relative importance of weak annihilation in traditional inclusive determinations of $|V_{ub}|$. Since few predictions have been made for the kinematics of weak annihilation, we explore a range of possibilities for WA, and ultimately present our results as a set of upper limits that vary with the kinematic properties of weak annihilation.

We compute a correction factor (aka "impact ratio") $R_a = \Gamma_{\mathrm{WA}}/\Gamma_{btou}$ that measures the relative contribution of WA for a given set $\{a\}$ of idealized cuts on $b \to u\,\ell\,\nu$ phase space. Not unexpectedly, we find that weak annihilation contributions in general must be quite small.

The results from the previous chapter are readily translated into a series of confidence intervals bounding the fractional size of WA contributions. Using the central values and total uncertainties computed by combining all contributions in quadrature, we compute symmetric 95% confidence intervals for the fractional impact of WA on the $b \to u\,\ell\,\nu$ rate, for each of the three analyses described in Ch 6.[1] For convenience, we halve these figures and report the impact on $|V_{ub}|$ as well. The results are presented in Tables 8.1–8.3.

8.2 Selected Results

The thirty different WA scenarios used in this study span a broad range of possible realizations of weak annihilation. Since little is known about the actual contribution from the WA term in the HQET expansion of the $b \to u\,\ell\,\nu$ rate, it is difficult to single out one particular sample as being most "representative" of weak annihilation. Given what we expect for the WA process, however, our broadest samples should in some sense be extreme variations, representing worse-

---

[1] We assume Gaussian statistics and take the upper and lower limits as $\mu \pm 1.96\,\sigma_{\mathrm{tot}}$ for central value μ with (Gaussian) total error σ_{tot}.

Table 8.1: Two-sided confidence intervals for R_{Endpt}. The 95% confidence intervals are computed using the total error evaluated in Ch 7 and reproduced in the third column above for reference. "L.L" indicates the lower limit; "U.L.", the upper limit. By halving the limits on the impact ratios, we obtain limits for the fractional impact on measurements of the CKM element $|V_{ub}|$ itself, shown in the final two columns.

			$\delta\Gamma/\Gamma$		$\delta\lvert V_{ub}\rvert/\lvert V_{ub}\rvert$	
Sample	R_{Endpt}	σ_{tot}	**L.L.**	**U.L.**	**L.L.**	**U.L.**
WA01	0.0614	0.0393	-0.016	0.138	-0.008	0.069
WA02	0.0356	0.0389	-0.041	0.112	-0.020	0.056
WA03	0.0208	0.0412	-0.060	0.102	-0.030	0.051
WA04	0.0190	0.0441	-0.067	0.105	-0.034	0.053
WA05	0.0295	0.0503	-0.069	0.128	-0.034	0.064
WA06	0.0477	0.0419	-0.034	0.130	-0.017	0.065
WA07	0.0248	0.0399	-0.053	0.103	-0.027	0.052
WA08	0.0163	0.0440	-0.070	0.103	-0.035	0.051
WA09	0.0203	0.0465	-0.071	0.111	-0.035	0.056
WA10	0.0373	0.0548	-0.070	0.145	-0.035	0.072
WA11	0.0300	0.0408	-0.050	0.110	-0.025	0.055
WA12	0.0179	0.0420	-0.064	0.100	-0.032	0.050
WA13	0.0164	0.0453	-0.072	0.105	-0.036	0.053
WA14	0.0215	0.0491	-0.075	0.118	-0.037	0.059
WA15	0.0450	0.0540	-0.061	0.151	-0.030	0.075
WA16	0.0338	0.0471	-0.058	0.126	-0.029	0.063
WA17	0.0281	0.0494	-0.069	0.125	-0.034	0.063
WA18	0.0308	0.0498	-0.067	0.128	-0.033	0.064
WA19	0.0456	0.0550	-0.062	0.153	-0.031	0.077
WA20	0.0639	0.0625	-0.059	0.186	-0.029	0.093
WA21	0.0391	0.0527	-0.064	0.142	-0.032	0.071
WA22	0.0392	0.0519	-0.063	0.141	-0.031	0.070
WA23	0.0437	0.0534	-0.061	0.148	-0.031	0.074
WA24	0.0653	0.0584	-0.049	0.180	-0.025	0.090
WA25	0.0754	0.0625	-0.047	0.198	-0.024	0.099
WA26	0.0481	0.0604	-0.070	0.167	-0.035	0.083
WA27	0.0529	0.0619	-0.068	0.174	-0.034	0.087
WA28	0.0797	0.0689	-0.055	0.215	-0.028	0.107
WA29	0.0767	0.0689	-0.058	0.212	-0.029	0.106
WA30	0.0906	0.0722	-0.051	0.232	-0.025	0.116

Table 8.2: Two-sided confidence intervals for R_{q^2,M_X}. See Table 8.1 or main text for details.

			$\delta\Gamma/\Gamma$		$\delta\lvert V_{ub}\rvert/\lvert V_{ub}\rvert$	
Sample	R_{q^2,M_X}	σ_{tot}	**L.L.**	**U.L.**	**L.L.**	**U.L.**
WA01	0.0286	0.0190	-0.009	0.066	-0.004	0.033
WA02	0.0166	0.0185	-0.020	0.053	-0.010	0.026
WA03	0.0099	0.0199	-0.029	0.049	-0.015	0.025
WA04	0.0097	0.0227	-0.035	0.054	-0.017	0.027
WA05	0.0175	0.0301	-0.042	0.077	-0.021	0.038
WA06	0.0222	0.0200	-0.017	0.061	-0.009	0.031
WA07	0.0116	0.0190	-0.026	0.049	-0.013	0.024
WA08	0.0080	0.0218	-0.035	0.051	-0.017	0.025
WA09	0.0108	0.0249	-0.038	0.060	-0.019	0.030
WA10	0.0231	0.0346	-0.045	0.091	-0.022	0.045
WA11	0.0142	0.0197	-0.024	0.053	-0.012	0.026
WA12	0.0087	0.0208	-0.032	0.049	-0.016	0.025
WA13	0.0085	0.0237	-0.038	0.055	-0.019	0.028
WA14	0.0121	0.0279	-0.043	0.067	-0.021	0.033
WA15	0.0301	0.0367	-0.042	0.102	-0.021	0.051
WA16	0.0183	0.0258	-0.032	0.069	-0.016	0.034
WA17	0.0158	0.0282	-0.039	0.071	-0.020	0.036
WA18	0.0188	0.0308	-0.042	0.079	-0.021	0.040
WA19	0.0304	0.0374	-0.043	0.104	-0.021	0.052
WA20	0.0504	0.0500	-0.048	0.148	-0.024	0.074
WA21	0.0250	0.0342	-0.042	0.092	-0.021	0.046
WA22	0.0262	0.0351	-0.043	0.095	-0.021	0.048
WA23	0.0312	0.0386	-0.045	0.107	-0.022	0.053
WA24	0.0512	0.0465	-0.040	0.142	-0.020	0.071
WA25	0.0685	0.0572	-0.043	0.181	-0.022	0.090
WA26	0.0398	0.0505	-0.059	0.139	-0.030	0.069
WA27	0.0453	0.0534	-0.059	0.150	-0.030	0.075
WA28	0.0723	0.0630	-0.051	0.196	-0.026	0.098
WA29	0.0743	0.0668	-0.057	0.205	-0.028	0.103
WA30	0.0974	0.0768	-0.053	0.248	-0.027	0.124

Table 8.3: Two-sided confidence intervals for R_{M_X}. See Table 8.1 or main text for details.

			$\delta\Gamma/\Gamma$		$\delta\lvert V_{ub}\rvert/\lvert V_{ub}\rvert$	
Sample	R_{M_X}	σ_{tot}	**L.L.**	**U.L.**	**L.L.**	**U.L.**
WA01	0.0164	0.0110	-0.005	0.038	-0.003	0.019
WA02	0.0095	0.0106	-0.011	0.030	-0.006	0.015
WA03	0.0057	0.0114	-0.017	0.028	-0.008	0.014
WA04	0.0055	0.0130	-0.020	0.031	-0.010	0.015
WA05	0.0100	0.0174	-0.024	0.044	-0.012	0.022
WA06	0.0127	0.0116	-0.010	0.035	-0.005	0.018
WA07	0.0066	0.0109	-0.015	0.028	-0.007	0.014
WA08	0.0045	0.0124	-0.020	0.029	-0.010	0.014
WA09	0.0061	0.0142	-0.022	0.034	-0.011	0.017
WA10	0.0132	0.0200	-0.026	0.052	-0.013	0.026
WA11	0.0081	0.0113	-0.014	0.030	-0.007	0.015
WA12	0.0050	0.0119	-0.018	0.028	-0.009	0.014
WA13	0.0049	0.0136	-0.022	0.031	-0.011	0.016
WA14	0.0069	0.0160	-0.024	0.038	-0.012	0.019
WA15	0.0173	0.0214	-0.025	0.059	-0.012	0.030
WA16	0.0104	0.0149	-0.019	0.040	-0.009	0.020
WA17	0.0090	0.0162	-0.023	0.041	-0.011	0.020
WA18	0.0107	0.0177	-0.024	0.045	-0.012	0.023
WA19	0.0175	0.0218	-0.025	0.060	-0.013	0.030
WA20	0.0292	0.0296	-0.029	0.087	-0.014	0.044
WA21	0.0143	0.0197	-0.024	0.053	-0.012	0.026
WA22	0.0150	0.0203	-0.025	0.055	-0.012	0.027
WA23	0.0179	0.0224	-0.026	0.062	-0.013	0.031
WA24	0.0296	0.0275	-0.024	0.084	-0.012	0.042
WA25	0.0400	0.0344	-0.027	0.107	-0.014	0.054
WA26	0.0230	0.0297	-0.035	0.081	-0.018	0.041
WA27	0.0263	0.0317	-0.036	0.088	-0.018	0.044
WA28	0.0426	0.0385	-0.033	0.118	-0.016	0.059
WA29	0.0438	0.0408	-0.036	0.124	-0.018	0.062
WA30	0.0582	0.0480	-0.036	0.152	-0.018	0.076

case scenarios in terms of the ease of distinguishing weak annihilation from the leading-order $b \to u\,\ell\,\nu$ rate, and measuring its impact on $|V_{ub}|$.

Guided by the intuition that the fundamental scale for WA effects is set by the QCD scale $\Lambda_{\rm QCD}$, we choose to distill the full results into a representative few by selecting from Tables 6.1–6.2 three characteristic WA samples that exhibit certain relevant kinematic properties:

- $\langle M_X \rangle \approx 2M_\pi \Rightarrow$ WA01, with $\langle M_X \rangle = 290$ MeV, $f_{2.2} = 0.999$.
- $\langle E_X \rangle \sim \Lambda_{\rm QCD} \approx 500$ MeV $\Rightarrow$ WA09, with $\langle E_X \rangle = 510$ MeV, $f_{2.2} = 0.929$.
- $\langle M_X \rangle \approx M_\rho \Rightarrow$ WA18, with $\langle M_X \rangle = 810$ MeV, $f_{2.2} = 0.453$.

These selected results are gathered together in Table 8.4. These numbers represent the essential distillation of this analysis.

Table 8.4: Distilled results for impact of WA effects on $b \to u\,\ell\,\nu$ rate and $|V_{ub}|$ measurements. Three representative WA samples have been chosen according to the characteristics labeled at the top of the six rightmost columns. For each set of experimental cuts, the 95% lower and upper limits on the indicated measurement is reported for each of the three samples. The first three rows of numbers show the limit on the relative size of the WA contribution to the $b \to u\,\ell\,\nu$ rate, and the second set show the impact on an extracted value for $|V_{ub}|$, obtained by simply halving the numbers in the upper rows.

		$\langle M_X \rangle \approx 2M_\pi$		$\langle E_X \rangle \sim \Lambda_{\rm QCD}$		$\langle M_X \rangle \approx M_\rho$	
	Analysis	**L.L.**	**U.L.**	**L.L.**	**U.L.**	**L.L.**	**U.L.**
$\delta\Gamma/\Gamma$	Endpt	-0.016	0.138	-0.071	0.111	-0.067	0.128
	q^2, M_X	-0.009	0.066	-0.038	0.060	-0.042	0.079
	M_X	-0.005	0.038	-0.022	0.034	-0.024	0.045
$\delta\lvert V_{ub}\rvert/\lvert V_{ub}\rvert$	Endpt	-0.008	0.069	-0.035	0.056	-0.033	0.064
	q^2, M_X	-0.004	0.033	-0.019	0.030	-0.021	0.040
	M_X	-0.003	0.019	-0.011	0.017	-0.012	0.023

8.2.1 Comparison to Previous Estimates

Projections for the impact on measurements of $|V_{ub}|$ are half as large as those for the impact on the rate, since $\Gamma_{btou} \propto |V_{ub}|^2$. As a point of comparison, we recall the work of Gibbons [2] (mentioned in Sec 3.5), which used a meta-analysis of several recent inclusive measurements to constrain a 1σ uncertainty on $|V_{ub}|$ due to WA effects to be less than $\pm 0.27 \times 10^{-3}$ on a central value for $|V_{ub}|$ of 4.63×10^{-3}, amounting to an upper limit at the 68% confidence level of 5.8%. The central value is from a recent combined inclusive q^2-M_X analysis carried out by the Belle collaboration [133].

Our new analysis of CLEO data improves the bound on the relative importance of WA for such a measurement. As a point of direct comparison, our 1σ (68%) upper limit is 1.8%, or in terms of a 95% confidence interval, we find[2]

$$\frac{\delta|V_{ub}|(\mathrm{WA})}{|V_{ub}|} < 3.0\% \qquad \text{at 95\% confidence.} \tag{8.1}$$

8.3 Statistical *vs.* Systematic Error

We note that in all cases, the central values for the fractional contribution of WA to the restricted $b \to u\,\ell\,\nu$ rate are not statistically significant. We also note that these measurements are dominated by their statistical errors, even after consideration of experimental systematics and dependence on the modeling of the $b \to u\,\ell\,\nu$ signal and $b \to c\,\ell\,\nu$ background.

As an alternative method of comparing the statistical and systematic errors, we present so-called “significance plots” in Fig 8.1 of the three yields N_{btoc}, N_{btou}, and N_{wkan}. The statistical significance is defined to be the ratio of the central value to the statistical error, and error bars are drawn to represent the relative size of the proportional total systematic error.

8.4 Speculation and Future Work

The results presented in this analysis are limited by the statistics of the CLEO II and II.V data samples. Inclusion of the ~6 fb^{-1} of e^+e^- data collected with the CLEO III detector collected at the $\Upsilon(4S)$ has the potential to reduce the statistical errors on our results by almost a third, and also offers the more tantalizing possibility of clarifying the small fluctuation seen in the data at high q^2 and lepton energy. We are considering an extension of this analysis to include the additional CLEO III data, providing the best constraint on WA that CLEO can extract from inclusive $B \to X_u\,\ell\,\nu$ decays.

Weak annihilation achieves its significance in part because of its potential to complicate experimental measurements of $|V_{ub}|$ in inclusive $B \to X_u\,\ell\,\nu$ decays. This thesis has explored the possible impact of WA on such measurements by

---

[2] The 68% and 95% upper limits we quote are for a q^2-M_X-style analysis, from the $\langle E_X \rangle \sim \Lambda_{\mathrm{QCD}}$ entry in Table 8.4.

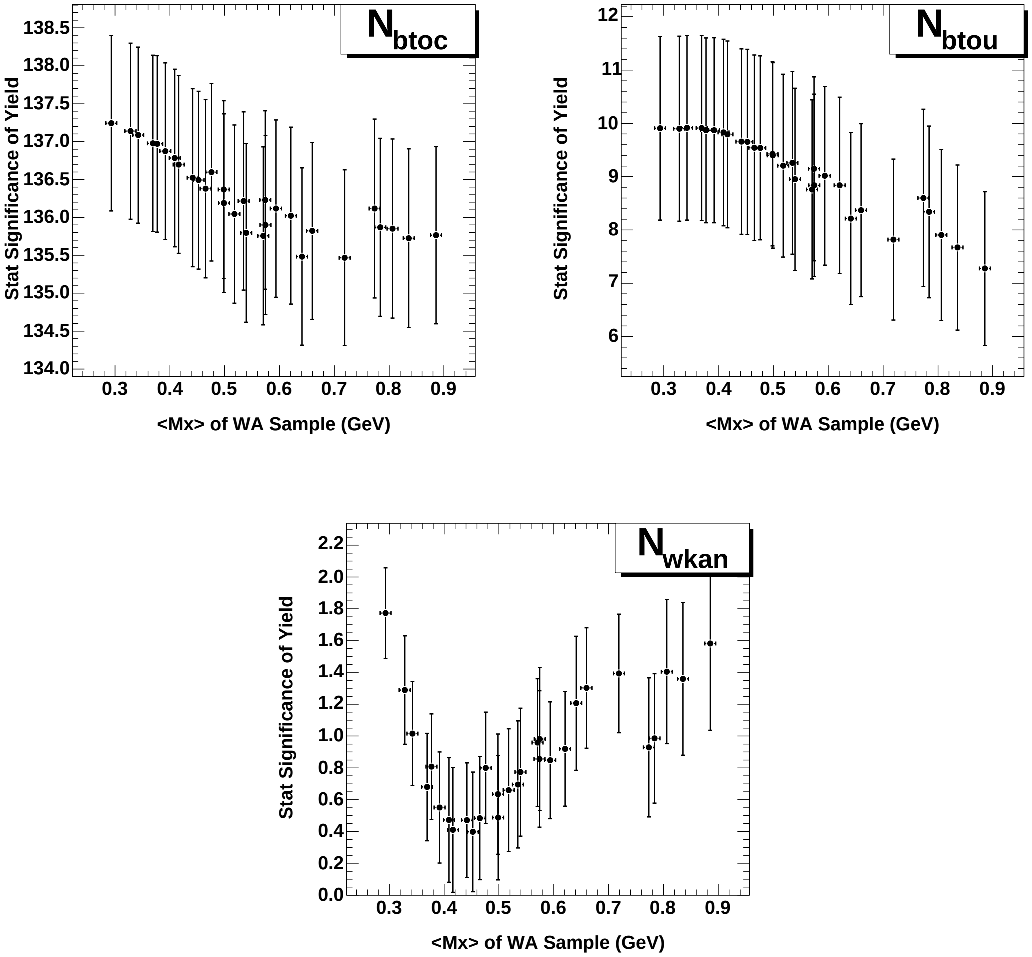

Figure 8.1: Statistical significance of fit yields. For each WA sample, we show the statistical significance of the fit yield, and draw error bars corresponding to the combined systematic error (detector $\oplus$ neutrino reconstruction $\oplus$ $b \to u$ $\oplus$ $b \to c$). Among other things, the plot allows for a ready comparison of the relative size between statistical and systematic errors.

looking directly at $b \to u\,\ell\,\nu$ decays in data, but there are other experimental avenues by which to investigate the possible contribution of weak annihilation. One such possibility is the comparison of the semileptonic decay rates of charged and neutral B mesons, perhaps most powerfully with a binning in q^2 to enhance identification of endpoint effects. Such an analysis necessarily requires information on the charge of the parent B, which is available through full or perhaps partial reconstruction of the signal B, or from features of the decay of the other B in the event. With the large data samples of $B\overline{B}$ events now available at the B factories, this possibility holds real promise for seeing conclusive evidence of weak annihilation, provided that systematics such as the precision on the ratio $\Gamma(\Upsilon \to$

$B^+B^-)/\Gamma(\Upsilon \rightarrow B^0\overline{B^0})$ do not prove to be limiting factors.

The charm sector is also sensitive to the same violation of QCD factorization that lies at the heart of weak annihilation in B decays. Studies of the semileptonic width of the D and the lifetime difference between the D and D_s mesons can help constrain the magnitude of such violations, as well as characterize the effects in a heavy-quark system. It is possible that the CLEO-c data now being taken at the $D\overline{D}$ threshold could also shed light on these issues.

Lastly, it may even be possible that progress in the simulation of QCD on the lattice will mitigate some of these problems in unexpected ways.

We optimistically predict that the almost inevitable theoretical and experimental progress on understanding of weak physics in general, and the $b \rightarrow u$ transition in particular, will deliver on the promise of a precision, well-constrained measurement of $|V_{ub}|$ within the decade.